Contrib Mineral Petrol (2004) 147: 705–721
DOI 10.1007/s00410-004-0579-x

ORIGINAL PAPER

R. Hugh. Smithies · David C. Champion · Shen-Su Sun

The case for Archaean boninites

Received: 1 October 2003 / Accepted: 1 April 2004 / Published online: 13 July 2004

Abstract Rare Archaean light rare earth element (LREE)-enriched mafic rocks derived from a strongly refractory mantle source show a range of features in common with modern boninites. These Archaean second-stage melts are divided into at least two distinct groups—Whundo-type and Whitney-type. Whundo-type rocks are most like modern boninites in terms of their composition and association with tholeiitic to calc-alkaline mafic to intermediate volcanics. Small compositional differences compared to modern boninites, including higher Al_2O_3 and heavy REE (HREE), probably reflect secular changes in mantle temperatures and a more garnet-rich residual source. Whundo-type rocks are known from 3.12 and 2.8 Ga assemblages and are true Archaean analogues of modern boninites. Whitney-type rocks occur throughout the Archaean, as far back as ca. 3.8 Ga, and are closely associated with ultramafic magmatism including komatiites, in an affiliation unlike that of modern subduction zones. They are characterised by very high Al_2O_3 and HREE concentrations, and their extremely depleted compositions require a source which at some stage was more garnet-rich than the source for either modern boninites or Whundo-type second-stage melts. Low La/Yb and La/Gd ratios compared to Whundo-type rocks and modern boninites either reflect very weak subduction-related metasomatism of the mantle source or very limited crustal assimilation by a refractory-mantle derived melt. Regardless, the petrogenesis of the Whitney-type rocks appears either directly or indirectly related to plume magmatism. If Whitney-type rocks have a boninitic petrogenesis then a plume related model similar to that proposed for the modern Tongan high-Ca boninites might apply, but with uniquely Archaean source compositions and source enrichment processes. Second-stage melts from Barberton (S. Africa –3.5 Ga) and ca. 3.0 Ga rocks from the central Pilbara (Australia) have features in common with both Whundo- and Whitney-types, but appear more closely related to the Whitney-type. Subduction zone processes essentially the same as those that produce modern boninites have operated since at least ~3.12 Ga, while a uniquely Archaean boninite-forming process, involving more buoyant oceanic plates and very inefficient mantle-source enrichment, may have occurred before then.

R. H. Smithies (✉)
Geological Survey of WA, 100 Plain Street,
East Perth, WA, 6004, Australia
E-mail: hugh.smithies@doir.wa.gov.au
Tel.: +61-9-92223611
Fax: +61-9-92223633

D. C. Champion · S.-S. Sun
Geoscience Australia, GPO Box 378, Canberra,
ACT, 2601, Australia

Introduction

Boninites are rare, water-rich, high-Mg basaltic to andesitic rocks. In the Phanerozoic record they are confined to convergent margin settings (Hickey and Frey 1982; Crawford et al. 1989). Intraoceanic arc, or fore-arc settings predominate, but boninites have also erupted in some young back-arc basins and occur even more rarely in continental arcs (Piercey et al. 2001). Their restricted occurrence reflects a very specific petrogenesis. Low TiO_2, high Al_2O_3/TiO_2 ratios (higher than primitive mantle values of ~21), and sub-chondritic Gd/Yb ratios reflect a mantle source that was refractory through one or more episodes of basaltic melt extraction (e.g., Sun and Nesbitt 1978). However, mantle normalised abundances of large ion lithophile elements (LILE), Th and La are typically high compared with those of high field strength elements (HFSE) and middle REE (MREE) (e.g., Gd). This is generally thought to reflect incompatible trace element enrichment of the refractory (previously melted) source by a subduction-derived fluid or melt immediately prior to remelting (i.e., second-stage melting) to form boninites, typically at low-pressure (< 50 km) and within anomalously hot suprasubduction zone conditions (Sun and Nesbitt 1978; Hickey and Frey

1982; Crawford et al. 1989; Falloon and Danyushevsky 2000).

These distinctive petrogenetic requirements mean that boninites strongly implicate modern subduction zone processes. As a result, boninites are potentially of great importance to Archaean granite-greenstone terrains in identifying successions that might be analogous to modern successions developed in subduction settings. Many models for Archaean crustal and tectonic evolution view greenstone terranes as various tectonic components (e.g., island arcs, back arc basins, oceanic plateaus) accreted at modern style subduction zones. These models should also predict the occurrence of Archaean boninites, perhaps even in a higher relative abundance than in modern settings, given the higher predicted Archaean mantle temperatures (e.g., Abbott and Hoffmann 1984; Bickle 1986). Indeed, there have been several accounts of rocks variously described as ''boninite-like'', ''boninite-type'' or ''boninite-series'' from Archaean sequences spanning the age range between ca. 3.8 and ca. 2.7 Ga (Kerrich et al. 1998; Boily and Dion 2002; Polat et al. 2002; Smithies 2002). Like modern boninites, most of the Archaean rocks have low TiO_2 and high Al_2O_3/TiO_2 and sub-chondritic Gd/Yb ratios, reflecting a strongly refractory source component, and they have LREE, Th, and LILE enrichments that are attributed to a subduction-enriched mantle source rather than to assimilation of felsic crust. Because of their strongly refractory source, we use the non-genetic term ''second-stage melts'' to collectively refer to these Archaean LREE-enriched rocks.

Polat et al. (2002) showed that rocks within the Garbenschiefer unit of metavolcanic amphibolites from the Central Tectonic Domain of the ca. 3.7–3.8 Ga Isua greenstone belt (southwest Greenland) were LREE-enriched second-stage melts. The rocks are intercalated with abundant ultramafic units, but because of extreme poly-phase deformation and high-grade metamorphism it is not clear whether the ultramafic rocks were originally extrusive or intrusive (Polat et al. 2002). These authors showed that the second-stage melts could have formed simply by mixing material compositionally equivalent to that of locally available South Isua tonalites with a refractory-mantle melt. They suggested, however, that this mixing occurred in the mantle source region rather than through assimilation of tonalitic crust during magma emplacement.

Parman et al. (2001, 2003) suggest that komatiites and komatiitic basalts from the ca. 3.5 Ga komati formation of the Barberton greenstone belt, South Africa, resulted from extensive melting of mantle that was more hydrous and at a lower temperature than is commonly thought appropriate for Archaean komatiites. These authors suggest that some komatiites and komatiitic basalts may be the Archaean equivalents of boninites. Arndt et al. (1998) and Arndt (2003a), however, show that the major- and trace-element compositions of these rocks are not consistent with melting above a hot Archaean subduction zone. Nevertheless, a small number of Barberton komatiitic basalts do contain very low TiO_2, high La/Gd and low Gd/Yb, with overall trace- and major-element compositions resembling those of modern boninites (Jahn et al. 1982; Sun et al. 1989; Parman et al. 2001, 2003).

Second-stage melts were emplaced as high-level sills during the evolution of the 2.97–2.95 Ga Mallina Basin in the central part of the Pilbara Craton, Western Australia (Smithies 2002). No broadly contemporaneous subduction is known from the region and so the origin of these rocks was compared to Palaeoproterozoic high-Mg norite dykes, many of which are thought to come from a subduction-modified refractory mantle that remelted during a post-subduction (by up to 500 m.y., Cadman et al. 1997; Tarney 1992) thermal event, commonly associated with the early stages of flood basalt magmatism (e.g., Hall and Hughes 1993; Cadman et al. 1997).

In the ca. 2.8 Ga Frotet-Evans greenstone belt of the Opatica sub-province, Superior Province, Canada, second-stage melts form lavas in a sequence dominated by tholeiitic basalt, that locally either overlies adakitic volcanics or is intercalated with calc-alkaline andesitic to rhyodacitic volcanics (Boily and Dion 2002). This occurrence of Archaean second-stage melts is notable for the absence of associated komatiites, and Boily and Dion (2002) interpret the package as having developed in a marginal oceanic basin following fore-arc rifting.

At a number of localities in the ca. 2.7 Ga Abitibi greenstone belt of the Superior Province, Canada, second-stage melts form lavas intercalated with both Al-depleted and Al-undepleted komatiites, and are locally also overlain by evolved arc tholeiites (Kerrich et al. 1998), forming an association interpreted as the products of subduction zone—plume interaction (Fan and Kerrich 1997; Kerrich et al. 1998; Wyman 1999; Wyman et al. 2002).

Siliceous high-Mg basalts (SHMB) (variably referred to as ''komatiitic'', ''komatiitic basalt'' or ''komatiitic andesite'') are a class of LREE-enriched, and relatively HFSE-depleted, igneous rocks that have been documented from a range of Archaean terrains (Arndt and Jenner 1986; Barley 1986; Sun et al. 1989; Riganti and Wilson 1995; Riganti 1996; Hollings and Kerrich 1999; Hollings et al. 1999) and that have been likened to modern boninites (Riganti and Wilson 1995). However, compared to both modern boninites and Archaean second-stage melts, SHMB typically have much higher TiO_2 (0.8 wt% cf. <0.5 wt%), Ti/Sc, and $(Gd/Yb)_{PM}$, and lower Al_2O_3/TiO_2 ratios (Table 1). The source of the SHMB clearly had not undergone the extent of prior melt depletion (if any) required of the source for either modern boninites or Archaean second-stage melts. While Riganti and Wilson (1995) suggested the Nondweni SHMB had boninitic affinities, a more detailed evaluation of these rocks (A. Riganti 1996; personal communication, 2004) concluded they were most likely komatiitic magmas that had assimilated felsic crust. This interpretation is consistent with previous

Table 1 Comparison of selected features of modern boninites, Archaean second-stage melts and siliceous high-magnesium basalts

	Modern boninites average (range)	Archaean magmas						
		Isua	Abitibi	Barberton	Mallina Basin	Opatica	Whundo	SHMB
SiO_2 (wt%)	56.8 (52.4–61.3)	49.6 (46.7–54)	49.6 (37.9–60.3)	50.8	53.2 (52.0–54.0)	52.0 (49.0–58.0)	50.2 (47.3–53.2)	53.2 (47.8–60.3)
Al_2O_3 (wt%)	10.6 (6.1–15)	17.6 (13.8–20.2)	18.1 (13.1–24.9)	13.0	17.2 (16.6–17.7)	14.4 (13.4–16.1)	16.5 (16.0–17.0)	9.92 (5.4–15.4)
TiO_2 (wt%)	0.2 (0.1–0.5)	0.3 (0.2–0.4)	0.3 (0.1–0.6)	0.3	0.3 (0.2–0.3)	0.4 (0.3–0.7)	0.3 (0.3–0.5)	**0.8 (0.4–2.4)**
MgO(wt%)	12.1 (4.5–21.7)	11.2 (6.7–16)	13.6 (6.1–24.5)	11.6	8.1 (7.8–8.6)	8.8 (5.7-13)	8.9 (8.1–9.9)	12.1 (3.8–21.6)
$Mg^{\#}$	65 (42–76)	67 (58–75)	71 (52–82)	69	64 (62–67)	63 (48–70)	63 (61–66)	64 (45–74)
Yb (ppm)	0.9 (0.3–2.4)	1.4 (0.9–1.8)	2.2 (1.2–3.6)	1.8	1.6 (1.5–1.7)	1.5 (1.1–2.4)	1.0 (0.6–1.6)	1.7 (1.0–2.8)
Zr (ppm)	20 (8–55)	19 (30–11)	22 (10–42)	45	37 (33–42)	38 (21–66)	26 (53–11)	**72 (22–181)**
Al_2O_3/TiO_2	67 (27–133)	66 (44–93)	70 (25–104)	42	66 (62–74)	33 (18–38)	50 (35–58)	**12 (5.5–26.4)**
Ti/Sc	31 (11–84)	45 (28–62)	34 (20–84)	40	40 (33–42)	No Sc data	45 (37–60)	**163 (100–263)**
$(La/Yb)_{PM}$	1.7 (0.4–6.0)	0.4 (0.2–0.8)	0.4 (0.2–0.7)	2.0	2.7 (2.4–3.0)	1.4 (1.0–1.9)	1.9 (1.2–2.6)	2.2 (1.0–6.0)
$(Gd/Yb)_{PM}$	0.9 (0.5–1.5)	0.5 (0.3–0.6)	0.4 (0.3–0.6)	0.7	0.6 (0.5–0.6)	0.8 (0.7–1.1)	0.8 (0.7–1.0)	**1.4 (1.1–1.6)**
$(Zr/Sm)_{PM}$	1.7 (0.4–3.8)	1.3 (1.0–2.2)	1.4 (1.1–2.9)	1.6	1.4 (1.37–1.45)	1.4 (0.9–2.2)	1.0 (0.7–1.1)	1.1 (0.6–2.0)
$(Yb/Sc)_{PM}$	0.9 (0.3–4.0)	1.3 (1.0–2.2)	1.4 (0.8–2.4)	1.3	1.3 (1.2–1.5)	No Sc data	0.7 (0.5–1.1)	**1.9 (1.1–3.3)**
Interpreted setting	Intraoceanic arc, fore-arc, rarely back-arc	Intraoceanic subduction zone	Convergent margin—subduction zone-plume interaction	Fore-arc	Intracratonic	Fore-arc rift	Arc (back-arc?)	Intraplate and subduction magmatism
Associated komatiites ?		Yes	Yes	Yes	No	No	No	Yes

Data source: Modern boninites = compilation in Smithies (2002), except for Yb, Ti/Sc, Yb/Sc and Zr/Sm, which are from the GEOROC database (see text): Archaean second-stage melts—from references detailed in the text: siliceous high-magnesium basalts (SHMB)—average of 130 samples from Sun et al. (1989), Riganti (1996), Hollings and Kerrich (1999), and Hollings et al. (1999)Values in *bold* in SHMB column highlight major compositional differences

(Arndt and Jenner 1986; Barley 1986; Sun et al. 1989) and subsequent (Hollings and Kerrich 1999; Hollings et al. 1999) studies, and while Smithies et al. (in press) note that similar rocks can be sourced from a subduction enriched (though not necessarily strongly refractory) source, the petrogenesis of SHMB is not considered relevant here.

In this study, we describe a new occurrence of Archaean second-stage melts from the 3.12 Ga Whundo Group, in the western part of the Pilbara Craton, Western Australia. Like the Opatica lavas, the Whundo lavas show no clear relationship to komatiite magmatism and form part of a generally tholeiitic and calc-alkaline basaltic sequence that is almost certainly arc related. The importance of the Whundo second-stage melts is twofold. First, their composition and magmatic association strongly suggest that modern style boninite magmatism did occur in the Archaean as far back as 3.12 Ga. Second, the similarities in composition and magmatic association to modern boninites can be used to highlight specific anomalies in most of the other documented Archaean second-stage melts. This suggests either that those rocks did not have a boninitic petrogenesis or that the petrogenesis of the Archaean equivalents of boninites had additional complications not seen within modern boninites.

The Whundo second-stage melts

The Whundo Group is preserved as a >10-km-thick sequence of mafic lavas and lesser andesitic to rhyodacitic volcaniclastic rocks, and minor ultramafic rock (Hickman 1997). It is fault bounded against older granite-greenstone terrane to the north and is unconformably overlain by ca. 3.0 and 2.7 Ga volcano-sedimentary sequences to the southeast. Felsic volcanic rocks form a minor component throughout the succession, and SHRIMP zircon dating on eight rocks provides a total apparent depositional age range of ca. 3,125–3,115 Ma (Nelson 1996).

Geochemically, the Whundo Group can be broadly divided into three packages; a lower package of calc-alkaline basalt and basaltic andesite lavas, a middle package of tholeiite and ferrotholeiite lavas, and an upper mixed package of tholeiite, calc-alkaline basalt to andesite and felsic volcaniclastic rocks. Second-stage melts form ~1–10 m thick pillowed flows within the basal part of the lowest calc-alkaline package, where they form less than ~20% of the outcrop. They also occur more rarely near the base of the middle tholeiite package. While ultramafic rock occurs within the lower part of the Whundo Group (Hickman 1997), it is not demonstrably volcanic or temporally related to the Whundo Group, and is not spatially associated with the second-stage melts.

Greenschist-facies metamorphism has resulted in recrystallisation of the second-stage melts to an assemblage dominated by actinolite, chlorite, serpentine,

epidote, calcite and talc, but original igneous textures are locally well preserved. These show the lavas to have been vesicular, extremely fine-grained, glass-rich, rocks containing phenocrysts of euhedral to sub-hedral olivine (now chlorite and serpentine), up to 1 mm in size, and acicular pyroxene (now actinolite).

Composition of the Whundo second-stage melts

Analyses of the Whundo second-stage melts are presented in Table 2. These lavas have SiO_2 contents between 47.3 and 53.2 wt% (anhydrous average ~52.2 wt%), MgO concentrations from 8.1 to 9.9 wt% and $Mg^{\#}$ from 61 up to 66. TiO_2 concentrations are low (0.3–0.5 wt%), while CaO and, particularly, Al_2O_3 are high. This results in high Al_2O_3/TiO_2 ratios of 35–58. The rocks show strong enrichments in LREE and Th over MREE to heavy REE (HREE) [$(La/Gd)_{PM} = 2.75$–1.87], with moderate relative depletions of Nb and Ta, slight Zr and Hf depletions, $(Gd/Yb)_{PM}$ between 0.98 and 0.66, and $(Yb/Sc)_{PM}$ from 1.14 to 0.47.

The second-stage melts are chemically distinct from their host calc-alkaline and tholeiitic lava sequences (Fig. 1). The lithological range, stratigraphy, and geochemistry of the entire Whundo Group (Smithies et al. in preparation), and a lack of intercalated terrigenous or continental sedimentary material, are consistent with some form of oceanic arc—possibly a rifted arc setting as suggested by Smith (2003).

Comparison between Archaean second-stage melts and modern boninites

The most significant similarities between modern boninites and Archaean second-stage melts are the low TiO_2 contents, low $(Gd/Yb)_{PM}$ and Ti/Sc ratios, and high Al_2O_3/TiO_2 ratios (Table 1)—all indicating a strongly refractory mantle source component. In modern basaltic rocks, steep arrays on a plot of Ti/Zr vs. Zr (Fig. 2), like those shown by the Archaean rocks, have also been explained in terms of prior melt extraction from a mantle source (Woodhead et al. 1993). Like modern boninites, the Archaean rocks show variable enrichments in LREE and Th. These enrichments have been attributed to a subduction-enriched mantle source (Kerrich et al. 1998; Boily and Dion 2002; Polat et al. 2002; Smithies 2002), but in only a few cases has the interpretation of a subduction environment for the host assemblages been corroborated by a range of independent lines of evidence (e.g., Kerrich et al. 1998; Boily and Dion 2002). These superficial similarities with modern boninites—a strongly refractory mantle source re-enriched in LREE and Th, and an interpreted subduction setting—clearly warrant further investigation in terms of a common petrogenesis. In this section, we compare the compositions of modern boninites with Archaean LREE-enriched second-stage melts. For modern boninites, the data includes ~350 analyses of fresh rocks from the GEOROC database (http://georoc.mpch-mainz.gwdg.de/). Typical analyses are shown in Table 2 and several compositional components are compared in Table 1.

The Archaean rocks are typically described as comprising various combinations of greenschist to amphibolite facies minerals including chlorite, clinozoisite, sericite, actinolite-tremolite and plagioclase (Kerrich et al. 1998; Polat et al. 2002; Smithies 2002). Polat et al. (2002) showed that during alteration and low-grade metamorphism of basaltic rocks, elements such as Al, Ti, REE, and HFSE are generally only weakly mobile. Hence the Al_2O_3/TiO_2 ratios observed for the Archaean second-stage melts can be considered primary. Kerrich et al. (1998), Boily and Dion (2002), Polat et al. (2002) and Smithies (2002) all note the consistency of REE and HFSE trends within individual suites of Archaean second-stage melts, suggesting that relative abundances of these elements have not been significantly altered.

While modern boninites and Archaean second-stage melts show extensive overlap in terms of some major elements, the SiO_2 range for the latter is to lower values than for modern boninite, whereas Al_2O_3 contents are higher, particularly in the Abitibi and Isua rocks (Table 1, Fig. 3). The rare Barberton second-stage melts are an exception here, showing relatively low concentrations of both SiO_2 and Al_2O_3. The range for the Opatica second-stage melts overlaps the range for modern boninites.

On primitive mantle normalised multi-element plots, Archaean second-stage melts show a wide range of trace-element abundances (Fig. 4), commonly with "U"-shaped patterns caused by depletions in Ti and MREE relative to Th, LREE and HREE. Compared to modern boninites, Archaean second-stage melts typically show significantly higher HREE concentrations, and consequently lower Gd/Yb (Fig. 5). The exceptions are some of the Whundo and Opatica lavas, which also have low HREE and relative high Gd/Yb ratios, similar to modern boninites.

Relatively high $(Zr/Sm)_{PM}$ ratios are a feature of many modern boninites (Fig. 6) and so the presence of such anomalies in many of the Archaean second-stage melts has been cited as strong evidence for a boninite-like petrogenesis (Parman et al. 2001; Boily and Dion 2002; Polat et al. 2002). It is important to note, however, that the high-Ca Tongan boninites show significant relative Zr (and Hf) depletions (Fig. 6). The field for Archaean second-stage melts actually lies between that for the Tongan boninites [$(Zr/Sm)_{PM} < 1$] and that for other modern boninites (mostly > 1.5). As a group, the Whundo rocks show the lowest $(Zr/Sm)_{PM}$ of the Archaean second-stage melts with values ~1.0.

A compositional feature perhaps more diagnostic of modern boninites is $(Yb/Sc)_{PM}$ ratios < 1. About 85% of modern boninites share this feature, with ratios > 1 almost exclusively restricted to the more fractionated rocks (Fig. 7). This feature can be explained in terms of

Table 2 Geochemistry of second-stage melts from the Whundo Group, and representative analyses of other Archaean second-stage melts and of Phanerozoic boninites

Unit (age)	Whundo (ca. 3.12 Ga)						Abitibi (ca. 2.7 Ga)		Opatica (ca. 2.8 Ga)		Mallina (2.95–2.97 Ga)		Barberton (3.49 Ga)	Isua (3.7–3.8 Ga)		Tonga (Phan.)				
Sample	174438	174440	174441	180232	174453	174456	PM2	NC-33	9312531	957304	142–194	142359	S-lc	462965	462903	IV 3–53	I 3–44	2981	106	B6
Major elements (wt%)																				
SiO_2	47.31	50.91	50.92	49.34	49.78	53.25	43.80	57.90	58.00	51.40	53.51	52.69	50.81	47.92	51.21	57.51	54.35	58.46	56.20	53.71
TiO_2	0.29	0.31	0.37	0.31	0.29	0.47	0.18	0.64	0.47	0.36	0.26	0.24	0.31	0.23	0.33	0.29	0.20	0.10	0.13	0.21
Al_2O_3	16.77	16.53	16.00	17.01	16.68	16.35	15.80	16.40	16.10	13.60	17.12	17.67	13.16	16.00	20.17	13.18	10.67	13.37	10.57	7.77
Fe_2O_3 T	10.33	10.65	10.69	10.44	9.77	10.11	11.20	11.10	7.20	10.70	9.01	8.48	11.44	10.80	10.96	10.25	10.46	9.19	8.94	10.14
CaO	7.91	6.80	6.95	6.87	8.41	8.43	6.68	3.57	9.40	10.50	8.11	7.41	10.43	9.82	5.81	9.53	8.66	8.11	7.44	4.64
MgO	9.95	8.80	9.36	8.32	9.12	8.13	22.00	6.14	6.10	10.70	8.22	8.64	11.96	13.56	8.47	8.14	14.99	9.39	11.19	18.49
MnO	0.20	0.19	0.15	0.22	0.21	0.20	0.21	0.17	0.10	0.20	0.16	0.17	0.15	0.21	0.14	0.18	0.19	0.00	0.16	0.17
K_2O	1.22	0.86	0.23	1.02	0.02	0.19	0.00	0.01	0.50	0.10 K	0.39	0.09	0.32	0.13	0.96	0.54	0.35	0.70	0.40	0.19
Na_2O	1.38	1.91	2.01	1.30	1.07	1.50	0.12	4.06	2.00	1.70	1.65	2.68	0.83	1.33	1.93	1.35	1.14	1.59	1.54	0.83
$P2O_5$	0.05	0.06	0.06	0.06	0.05	0.08	0.03	0.06	0.02	0.03	0.05	0.04	0.05	0.01	0.02	0.06	0.03	0.00	0.02	0.03
LOI	5.38	3.79	4.09	5.92	5.30	2.01	5.39	6.23	0.80	1.30	2.15	2.48	1.11	3.32	3.34	-0.07	0.05	3.92	3.95	4.32
$Mg^{\#}$	66	62	63	61	65	61	80	52	63	66	64	67	67	71	60	61	74	67	71	78
Trace elements (ppm)																				
Sc	42	49	42	51	43	47	48	46			36	43	47	45	34	50	50	36	38	24
V	125	133	133	162	131	144	170	240			163	158	193	229	195	275	247	174	181	136
Cr	259	89	188	190	164	158	1460	74			154	680	3001	1240	85	365	1095	538	695	1930
Co							74	80			59	54	99	77	50			37		
Ni	99	71	79	81	81	68	760	200			75	125	1039	455	101	84	275	140	194	540
Rb	56.00	37.00	5.80	35.80		5.40			20.00	11.00	14.63	5.62	12.20	3.20	44.40	8.00	6.00	12.20	9.00	
Sr	99	84	91	64	69	96			203	73	199	140	45	52	89	202	151	97	61	63
Ba	160	106	36	106	30	48			145		68	80	49	14	147	140	106	30	30	30
Y	4	10	10	6	6	15	9	24	11	13	12	11	15	9	11	9	7	5	5	4
Zr	11	33	27	13	16	53	12	42	59	24	38	33	36	14	25	17	12	25	20	30
Nb	0.30	1.60	1.60	0.80	0.80	2.90	0.42	1.90	1.20	0.90	1.42	1.11	1.47	0.13	0.62	1.00			1.00	
Th	0.20	0.60	0.60	0.20	0.20	1.00	0.05	0.30	0.72	0.33	0.84	0.77	0.62	0.04	0.27	0.82	0.48		0.10	
U		0.16	0.15	0.05		0.24		0.16	0.21	0.10	0.25	0.20	0.15							
La	1.39	3.82	3.20	1.32	2.18	5.89	0.49	2.40	3.35	1.90	6.46	5.16	3.79	0.31	1.39	3.94	1.77	1.27	0.82	2.50
Ce	3.74	9.56	7.92	2.99	4.39	14.38	1.33	6.26	7.01	4.20	12.50	10.28	7.79	0.86	3.41	7.95	4.10	2.57	1.79	5.46
Pr	0.50	1.21	1.03	0.43	0.58	1.85	0.21	0.88	0.93	0.55	1.47	1.23	0.93	0.14	0.48	0.94			0.27	0.61
Nd	2.18	5.14	4.35	1.92	2.62	7.72	1.11	4.27	3.58	2.50	5.42	4.58	3.83	0.76	2.27	4.47	2.85	1.65	1.20	2.84
Sm	0.63	1.22	1.24	0.52	0.58	1.88	0.39	1.37	1.04	0.76	1.09	0.91	0.97	0.35	0.73	1.31	0.82	0.43	0.35	0.75
Eu	0.27	0.35	0.41	0.25	0.24	0.51	0.14	0.43	0.41	0.33	0.33	0.24	0.32	0.19	0.22	0.49		0.15	0.11	0.24
Gd	0.60	1.28	1.37	0.61	0.69	1.95	0.63	1.92	1.51	1.20	1.17	0.98	1.33	0.61	1.04	1.34	1.27		0.40	0.74
Tb	0.10	0.25	0.24	0.09	0.11	0.34	0.14	0.43	0.28	0.25	0.21	0.19	0.28	0.14	0.20			0.10	0.08	0.13
Dy	0.64	1.51	1.52	0.77	0.79	2.15	1.32	3.55	2.07	1.70	1.51	1.40	2.09	1.25	1.62	1.67	1.16		0.60	0.79
Ho	0.14	0.33	0.34	0.18	0.18	0.48	0.36	0.94	0.45	0.40	0.39	0.38	0.52	0.35	0.42				0.14	0.16
Er	0.46	1.07	1.07	0.57	0.61	1.44	1.23	3.06	1.43	1.20	1.23	1.19	1.63	1.29	1.46	1.19	0.80		0.44	0.47
Tm							0.22	0.50	0.22	0.21	0.22	0.21		0.20	0.21					
Yb	0.60	1.27	1.23	0.77	0.78	1.63	1.49	3.42	1.40	1.40	1.54	1.52	1.83	1.37	1.44	1.19	0.86	0.59	0.52	0.48
Lu	0.10	0.20	0.20	0.16	0.13	0.24	0.24	0.52	0.22	0.22	0.27	0.26	0.28	0.21	0.22			0.10		

Analyses of Whundo Group rocks preformed at Geoscience Australia by XRF (major elements) and ICP-MS (trace-elements) using techniques described in Smithies et al. (in press)
Data sources: Abitibi, Kerrich et al. (1998); Opatica, Boily and Dion (2002); Mallina, Smithies (2002); Barberton, S. Parman, personal communication, (2003); Isua—Polat et al. (2002); Phanerozoic boninites – Cameron et al. (1983), Falloon and Crawford (1991), Hickey and Frey (1982)

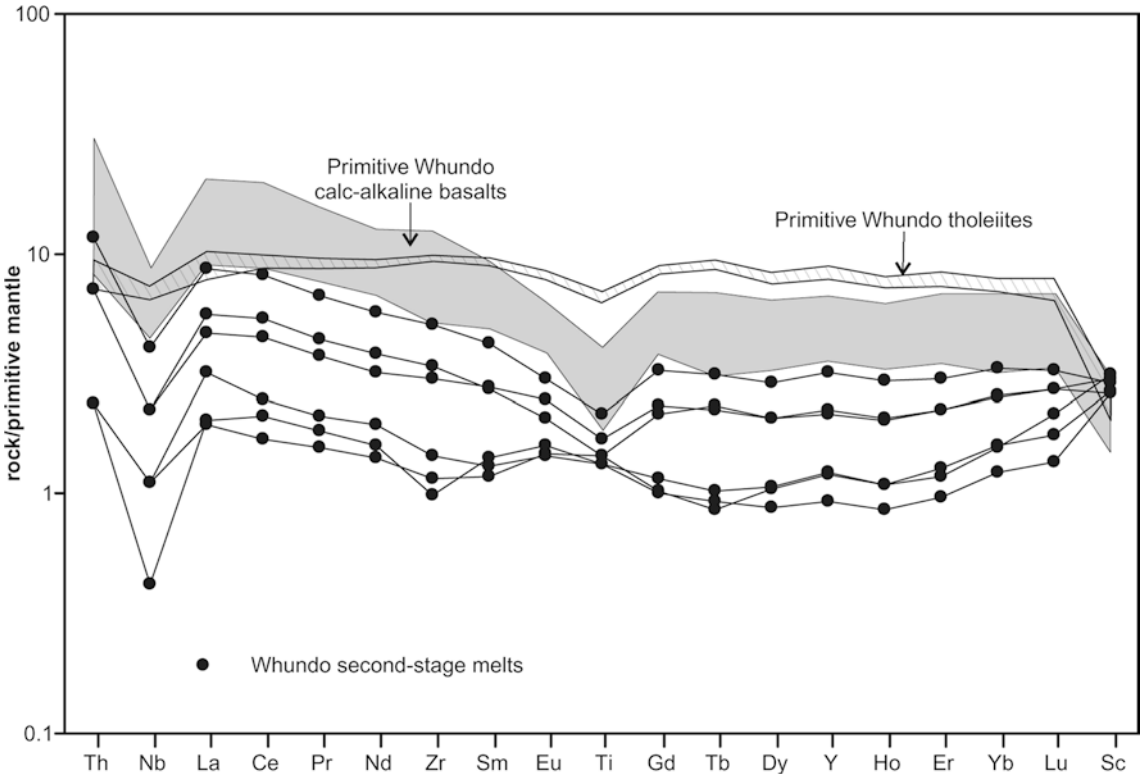

Fig. 1 Primitive mantle normalized trace element patters for second-stage melts from the ca. 3.12 Ga Whundo Group, of the western Pilbara Craton. Also shown for comparison are ranges for associated tholeiitic basalt and calc-alkaline basalt and andesite of the Whundo Group (unpublished data) (primitive mantle normalizing factors of Sun and McDonough 1989)

the roles of clinopyroxene and garnet; both were significant phases in the mantle source component during first-stage melting and the resulting low Yb/Sc signature was past to magmas produced during second-stage melting as both minerals were completely exhausted. In contrast, very few Archaean second-stage melts have low $(Yb/Sc)_{PM}$, with values approaching one found mainly in rocks with higher $Mg^{\#}$. The Whundo rocks are an exception with all but one having $(Yb/Sc)_{PM}$ between 0.96 and 0.54; no Sc data are reported for the Opatica second-stage melts. The high $(Yb/Sc)_{PM}$ in most of the Archaean rocks is not due to the higher HREE alone (Fig. 7) since many of these rocks also show a high concentration of Sc. Importantly, some Whundo lavas have high-Yb concentrations in the same range as the other Archaean rocks but still have $(Yb/Sc)_{PM} \sim 1$—at lower $Mg^{\#}$.

Features that distinguish many of the Abitibi second-stage melts from other Archaean second-stage melts are high Nb/La and Nb/Th ratios of 0.75–1.13 and 6–11, respectively; significantly higher than those expected from magmas derived from subduction modified mantle. Modern boninites and the other Archaean second-stage melts typically have Nb/La ratios < 0.5 and Nb/Th ratios < 4. Although Nb/La > 0.9 have been reported for some modern boninites, in most of these cases the very low Nb concentrations ($\sim$1 ppm or less) were determined by XRF and are regarded as unreliable (e.g., Cameron et al. 1983).

Two types of Archaean LREE-enriched second-stage melts

While general features such as low SiO_2 and high Al_2O_3 and Yb appear to distinguish most Archaean second-stage melts from modern boninites, there are also compositional features that separate the Archaean rocks into at least two types (Fig. 5). In particular, the Abitibi and Isua rocks have La/Yb < 1 and Gd/Yb < 0.8 and are referred to here as the Whitney-type [named after occurrences described by Kerrich et al. (1998) from near Whitney Township, Ontario]. In contrast, the Whundo and Opatica rocks have higher La/Yb and Gd/Yb and share these features with nearly all modern boninites; these Archaean rocks are referred to here as Whundo-types. The variations between the two types are not simply due to higher Yb in the Whitney-type, since the range for the Opatica rocks overlaps the upper end of the range for the Isua rocks. Further, both groups commonly have Yb concentrations greater than those of most modern boninites ($> \sim$1.5 ppm). The Mallina Basin and Barberton second-stage melts share characteristics of both groups. They have low, Whitney-type, Gd/Yb ratios, but Whundo-type Al_2O_3 concentrations and La/Gd ratios.

The Whitney- and Whundo-types show distinctive enrichment patterns for the highly incompatible trace elements. All Whundo-type rocks show systematic normalised increases from Sm to Th, with the exception of

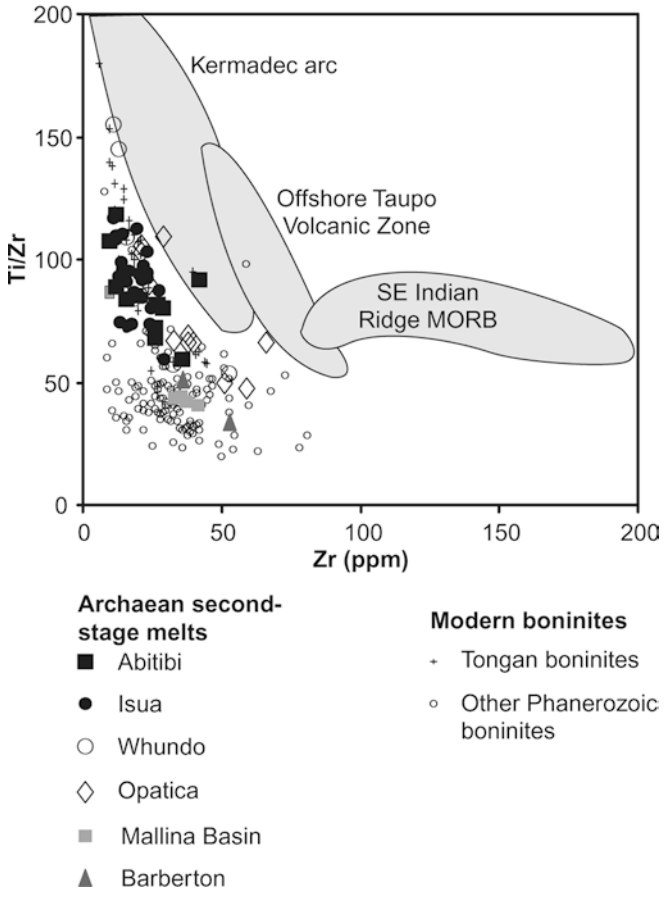

Fig. 2 Variation diagram showing Zr vs. Ti/Zr. Fields are from Gamble et al. (1995) and references therein, and compare suites showing steep arrays interpreted to reflect prior extraction of melt from a source (Kermadec, Offshore Taupo, with suites derived from less depleted sources (flat arrays—e.g., SE Indian MORB) Data sources for Archaean rocks include Jahn et al. (1982), Kerrich et al. (1998), Wyman et al. (1999), Boily and Dion (2002), Polat et al. (2002), Smithies (2002), and S. Parman, personal communication. Modern boninite data are from the GEOROC database (see text)

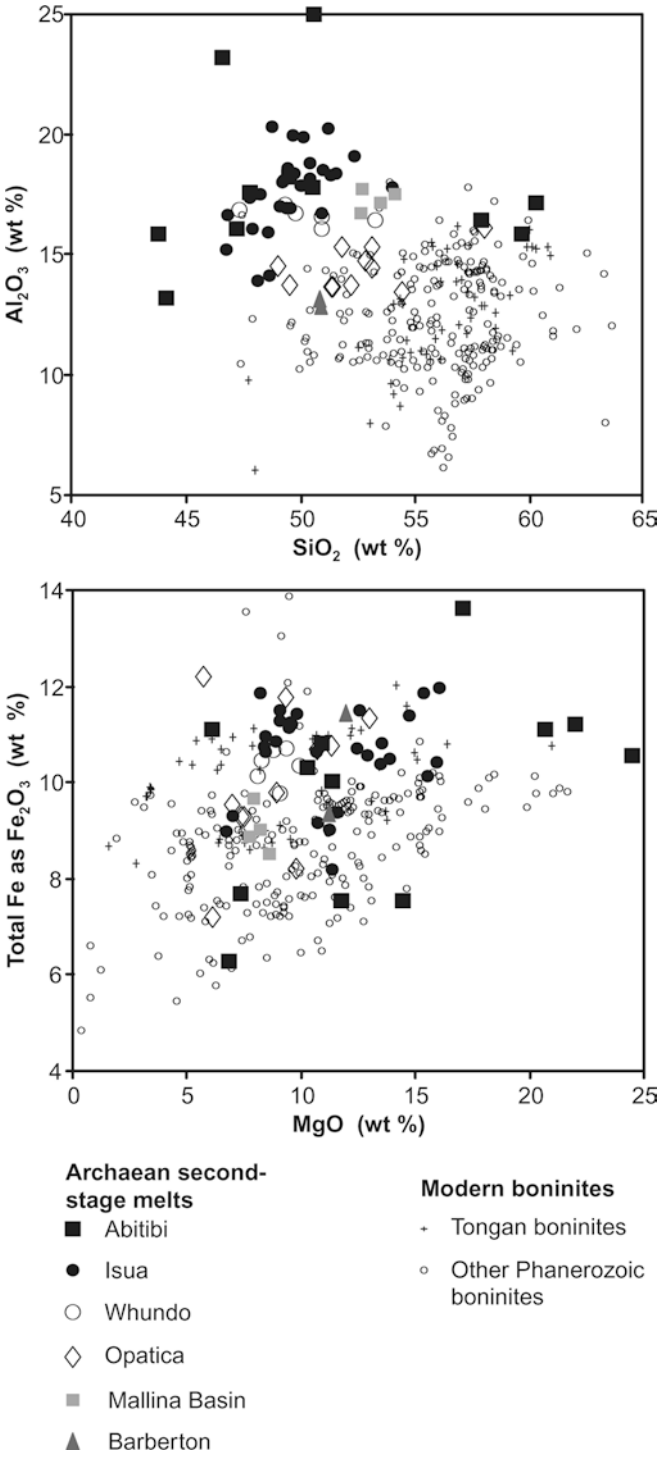

Fig. 3 Al_2O_3 vs. SiO_2 and Total Fe vs. MgO variation diagrams comparing Archaean second-stage melts to modern boninites (symbols as for Fig. 2)

negative Nb(Ta) anomalies (Fig. 4). In contrast, enrichment of the primitive members of the Whitney-type is much more subtle. The Isua rocks also show significant depletions in Nb with respect to NMORB and to Th and LREE, although the extent of Nb depletion in the Abitibi rocks is considerably less. Woodhead et al. (1998) point out that experimental and observational evidence does not favour the presence of Nb-rich residual phases during mantle melting, at least in the case of subduction-related mantle-derived magmas. If this conclusion is also relevant to the petrogenesis of the Archaean Whitney-type rocks, then the Nb depletion in the Isua rocks reflects significant relative enrichment in LREE and Th (though less than in the Whundo-type). In the case of the Abitibi rocks, either the unenriched mantle component was less LREE, Th and Nb depleted than was the case for the Isua rocks or the mantle source component was enriched by a component with low La/Nb and Th/Nb ratios. Alternatively, these low La/Nb and Th/Nb ratios may reflect a source component derived from a mantle plume, as has been suggested for the Tongan high-Ca boninites (Danyushevsky et al. 1995).

Kerrich et al. (1998) suggested the source for the Abitibi rocks (Whitney-type) was significantly less

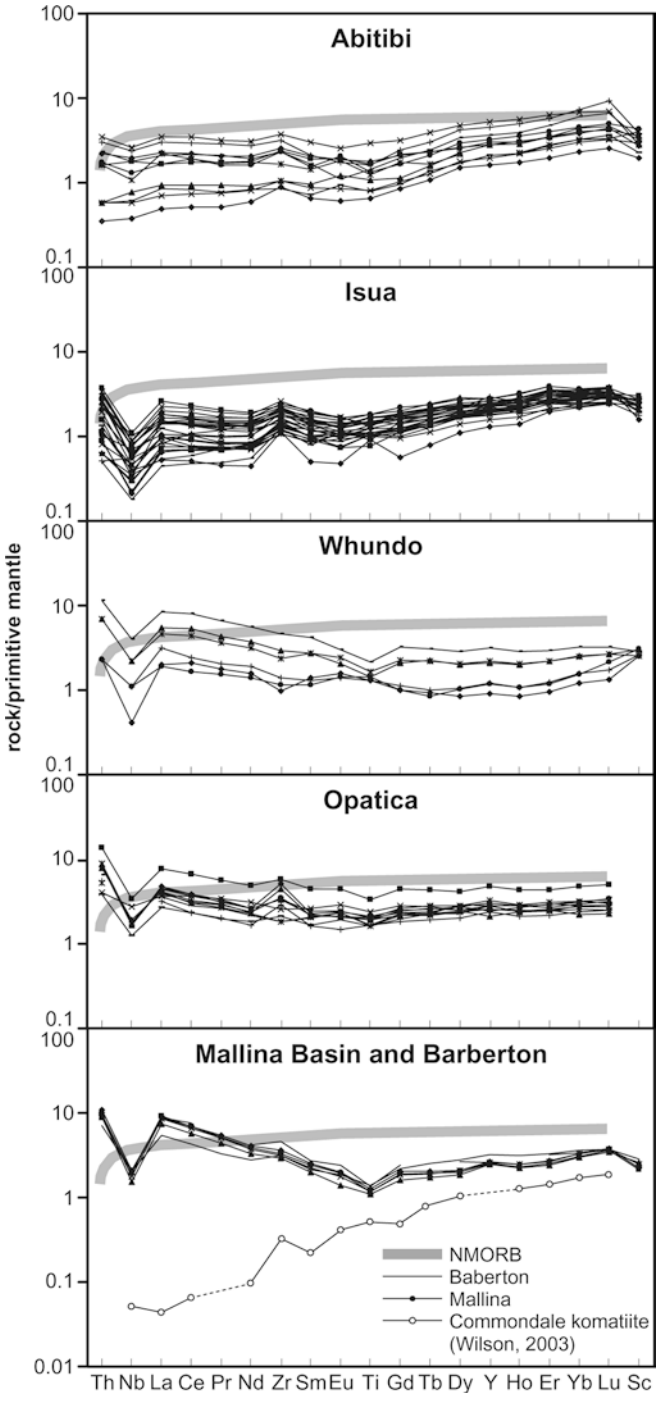

Fig. 4 Primitive mantle normalized trace element patters for Archaean second-stage melts (primitive mantle normalizing factors and NMORB values of Sun and McDonough 1989)

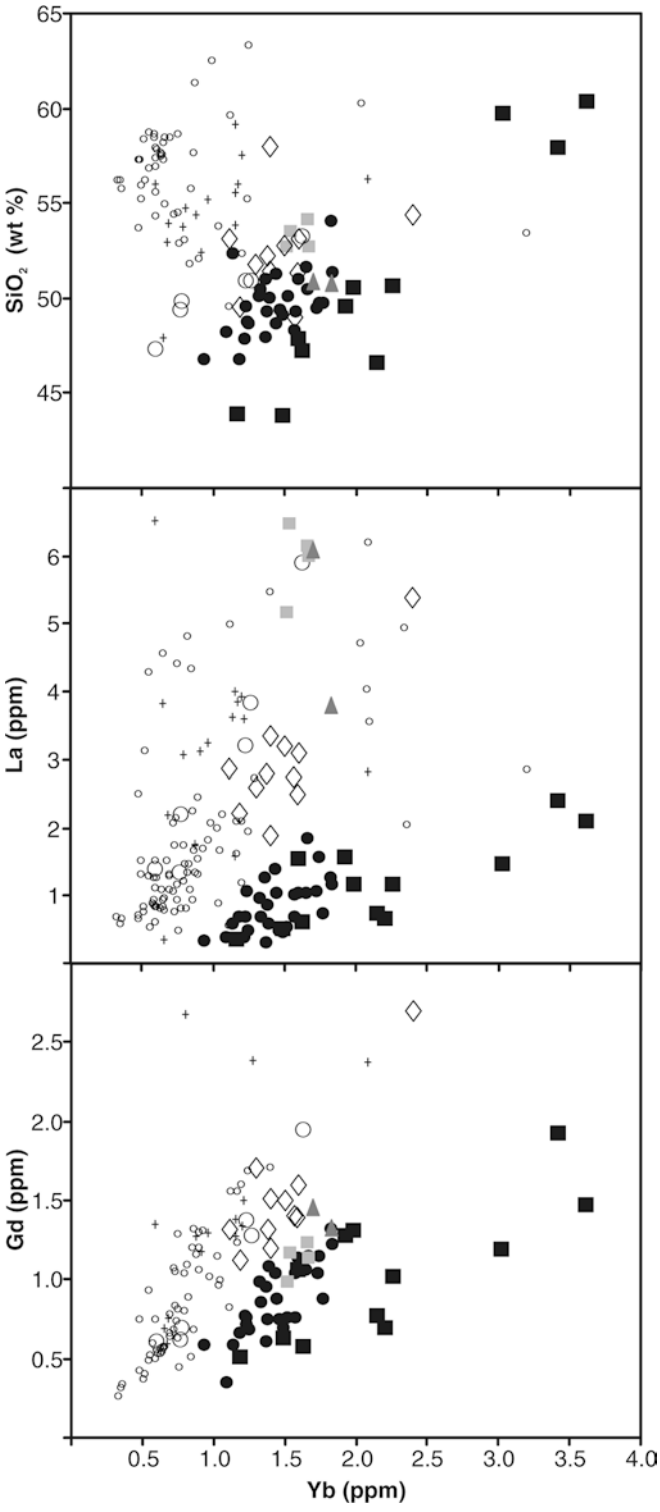

Fig. 5 Variation diagrams showing Yb vs. SiO_2, La and Gd (symbols as for Fig. 2)

enriched by a LREE-rich subduction-derived metasomatic component than was the source for most modern boninites. The clear compositional separation between the Whitney-type and Whundo-types in terms of La/Yb, however, suggests additional processes might have operated. The lower Gd/Yb in the Whitney-type rocks, compared to the Whundo-type rocks and modern boninites, cannot be attributed to lower degrees of metasomatic source enrichment since very low MREE and HREE concentrations in both slab-fluids and slab-melts (e.g., Hawkesworth et al. 1993a, 1993b; Martin 1999) should have little affect on mantle values. Modern boninites typically have Gd/Yb ratios >0.8 with ratios

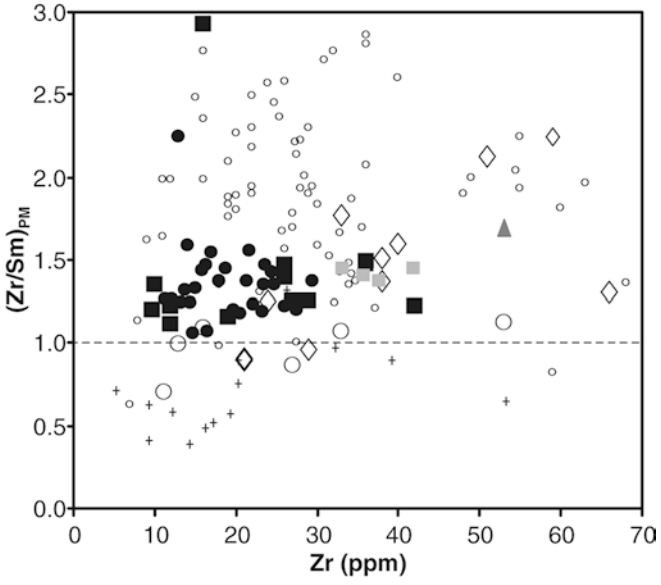

Fig. 6 Variation diagram showing Zr versus primitive mantle normalized Zr/Sm ratio (symbols as for Fig. 2)

as low as 0.7 being extremely rare. In contrast, the Gd/Yb ratio of the Whitney-type rocks ranges between 0.31 and 0.77, possibly identifying a source component rarely, if ever, seen in modern boninites or in the Whundo-type.

Compared to the Whundo-type, the Whitney-type samples typically have higher Al_2O_3 and Al_2O_3/TiO_2 even at equivalent $Mg^{\#}$ (Fig. 8). Distinctions also exist in the geological setting or association of the two groups. The Whitney-type form parts of sequences that include komatiites or are at least closely associated with ultramafic magmas (Kerrich et al. 1998; Polat et al. 2002). The Whundo-type rocks appear unrelated to komatiitic volcanism, forming parts of volcanic sequences that closely resemble modern subduction-related sequences (e.g., Boily and Dion 2002; Smithies et al. in preparation).

The Whundo-type also show a large range in Th/Yb and La/Yb ratios that are sensitive to variation in degrees of partial melting, source enrichment or crustal assimilation, but comparatively small variations in $Mg^{\#}$. The opposite, however, is true for the Whitney-type (Fig. 8). The most obvious explanation for this is that compositional variation in the Whitney-type is strongly influenced by fractional crystallisation, while varying degrees of refractory source melting had a more significant control on compositional variation within the Whundo-type.

The refractory source component

The typically higher ΣFe (Fig. 3) in modern high-Ca boninites and in Archaean second-stage melts (Whitney- and Whundo-types) suggests a less refractory source for these rocks than for modern low-Ca boninites. Ratios of moderately to only weakly incompatible elements (e.g.

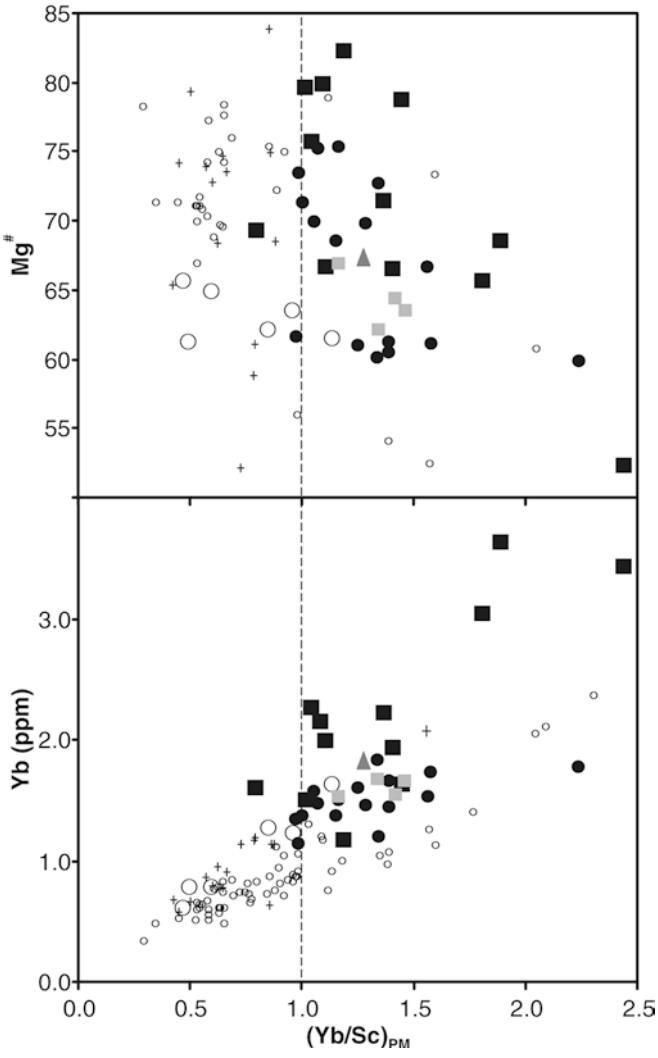

Fig. 7 Variation diagram showing primitive mantle normalized Yb/Sc ratio vs. $Mg^{\#}$ and Yb (symbols as for Fig. 2)

Ti, HREE, Al, Sc, V) help define the nature of this refractory source component.

Typically high V and Sc in high-Ca boninites suggests clinopyroxene was present in the refractory mantle source but was exhausted, or nearly so, during melting and was not a significant phase during subsequent fractional crystallisation. The low V and Sc concentrations typical of modern low-Ca boninites (Fig. 9), on the other hand, suggest clinopyroxene was probably never a significant residual phase, either in production of the refractory harzburgitic mantle source or during subsequent boninite formation.

Compared to modern boninites, variation in V and Sc appears decoupled in the Archaean second-stage melts, implicating a mineral with a high $D^{Sc/V}$ (e.g., garnet). The high-Yb concentrations and high-Yb/Sc ratios of the Whitney-type rocks might imply variably lower degrees of partial melting than is the case for modern boninites. However, the associated high Sc and Al_2O_3 and low Gd/Yb are more consistent with melting out of

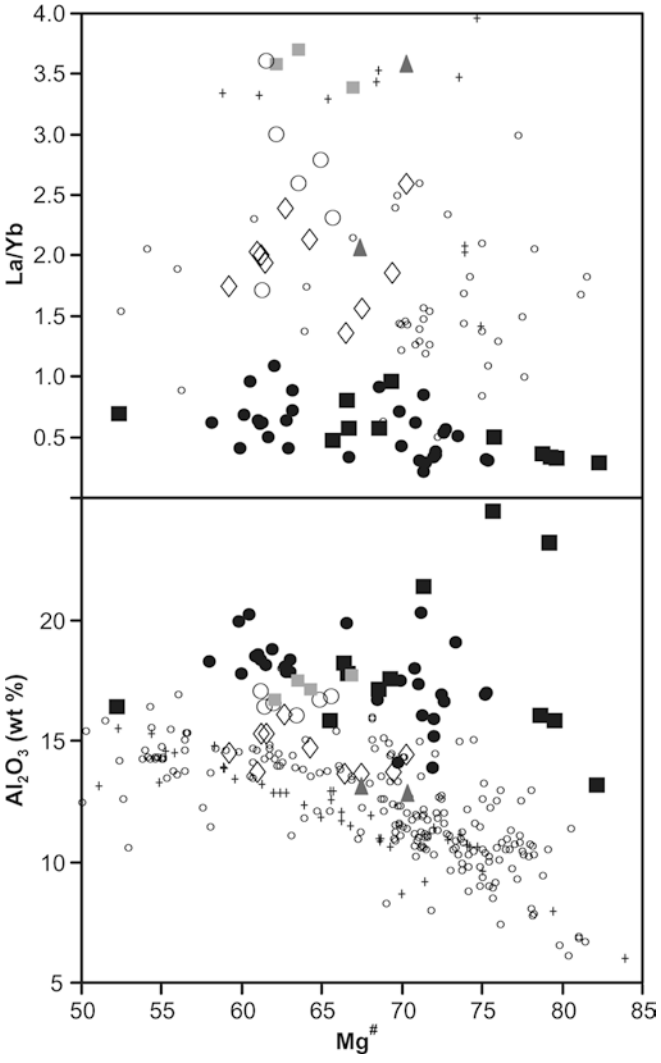

Fig. 8 Variation diagram showing $Mg^{\#}$ vs. Al_2O_3 and La/Yb (symbols as for Fig. 2)

garnet from an initially garnet-rich refractory source. In these rocks, higher $(Yb/Sc)_{PM}$ than is typical of modern boninites is consistent with residual clinopyroxene, or clinopyroxene fractionation. The Whundo-type rocks usually have Gd/Yb ratios and Al_2O_3 contents that lie between those of the Whitney-type and modern high-Ca boninites (Figs. 3 and 5), probably suggesting a slightly less garnet-rich source compared to the source for the Whitney-type rocks. It is most likely that this garnet was residual from an early melt-depletion event, but was subsequently eliminated during or before boninitic magma production. Certainly, the trace-element composition of the Archaean rocks indicates that no garnet remained in the source after second-stage melting, thus pointing to lower-pressure origin.

Origins of variable Zr/Sm ratios

High $(Zr/Sm)_{PM}$ in most modern low-Ca boninites has been explained in terms of residual amphibole (low

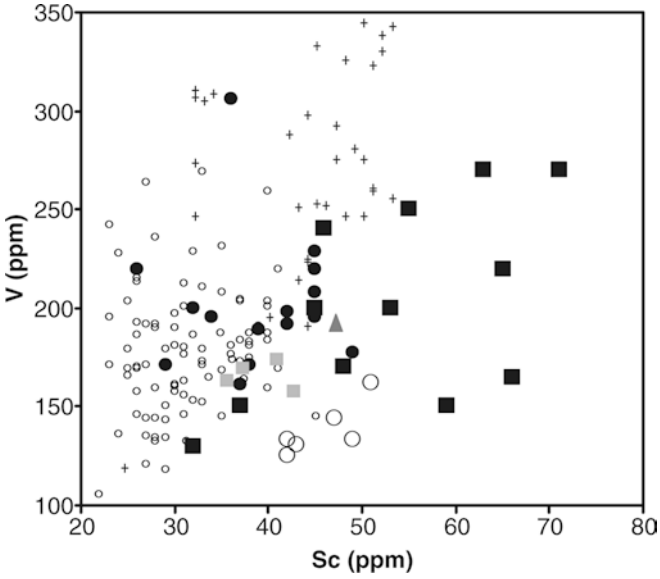

Fig. 9 Variation diagram showing Sc vs. V (symbols as for Fig. 2)

$D^{Zr/Sm}$) during production of boninite or one of its source components (Hickey and Frey 1982). If this is the case then the low $(Zr/Sm)_{PM}$ of the Tongan high-Ca boninites likely reflects the instability of amphibole under the particularly high mantle melting temperatures required to produce high-Ca boninites (e.g., ~1,480°C, Falloon and Danyushevsky 2000). It seems most likely that garnet ($D^{Zr/Sm}$ ~1.8, Suhr et al. 1998), rather than amphibole, was stable during production of the Tongan boninites or one of the source components (e.g., an eclogitic residual for a slab-derived metasomatic component).

The ultra-depleted Archaean Commondale komatiites, from South Africa, (Wilson et al. 2003, Wilson 2003) present an interesting case of ultramafic lavas derived from a strongly refractory source that was not noticeably enriched in trace elements (except perhaps water), prior to melting. The rocks, nevertheless, show high $(Zr/Sm)_{PM}$ (~1.2–1.5, Fig. 4) which must relate to mantle source mineralogy rather than to metasomatic enrichment. It is possible that melting at pressures high enough to leave significant residual garnet would result in a refractory source having $(Zr/Sm)_{PM} > 1$. If remelting of that source consumes all garnet, or occurs at pressures below the stability range of garnet, as suggested for the Whitney-type rocks in particular, the resulting liquids will inherit the high $(Zr/Sm)_{PM}$; this ratio would be further enhanced by residual clinopyroxene, which, like amphibole, has a low $D^{Zr/Sm}$ (~0.3, Suhr et al. 1998; Green et al. 2000).

Trace element modelling

Trace element enrichments in some Archaean basalts are the result of crustal assimilation (e.g., Arndt and Jenner 1986). We performed simple mixing calculations to see if

incorporation of crustal material into a hypothetical melt of refractory mantle, with or without subsequent fractionation of mantle phases (AFC, De Paolo 1981), could also approximate the trace-element patterns of various *primitive* Archaean second-stage melts. The hypothetical refractory-mantle derived melt was assumed to have Yb and Nb concentrations slightly less than that of primitive Archaean second-stage melt (primitive Isua rock in the case of the Whitney-type and primitive Opatica rock in the case of the Whundo-type). Other trace-element concentrations were estimated by extrapolation, assuming systematically-decreasing primitive mantle-normalised REE and HFSE abundances between Yb and Nb. Crustal compositions used in the modelling include average Archaean Pilbara Craton granite (R.H. Smithies and D.C. Champion, unpublished data), average Archaean crust (Taylor and McLennan 1985), average trondhjemite (Barker et al. 1979; Davis et al. 1994; Li and Li 2003), and average adakite (Drummond et al. 1996). Partition coefficients used are those quoted by Suhr et al. (1998) except for Nb, for which the values from Green et al. (2000, run 1,802) were used. The values used for clinopyroxene and garnet are similar to those obtained by Gaetani et al. (2003). Details of trace element modelling are presented in Table 3 and results are presented in Table 4 and Fig. 10.

The Whitney-type rocks have very low LREE concentrations. Accordingly, even extremely small amounts of assimilated felsic crust (< 0.1% average Pilbara granite; < 0.5% average Archaean crust) produce unreasonably high-La/Nd ratios in modelled parental magma (unless the refractory-mantle melt component had unusually low La/Nd ratios). Fractional crystallisation of clinopyroxene from the hypothetical refractory-mantle melt (model 1, Fig. 10), with no assimilation of crust, produces *primitive* Whitney-type REE patterns but not the positive Zr and the negative Nb anomalies, and the extensive fractionation (70%) required is not consistent with the high $Mg^{\#}$ and Sc concentrations in the primitive rocks.

The suggestion that assimilation of felsic crust is unlikely is consistent, in the case of the Abitibi rocks, with an oceanic geological setting (Kerrich et al. 1998). With the exception of variable Nb anomalies, the primitive Abitibi and Isua rocks show very similar trace element patterns, suggesting a common petrogenesis. Unless melting of the mantle source for the Isua rocks left a residual Nb-rich phase, the significant normalised negative Nb-anomalies within the Isua rocks (and less so in the Abitibi rocks) reflects some form of enrichment. The implication is that the enriched component in the case of the Abitibi rocks had a much lower La/Nb than in the case of the Isua rocks.

Assimilating ~10–15% of either adakitic material or average Archaean crust reproduces Whundo-type trace element patterns reasonably well (model 2, Fig. 10), and adding ~10% trondhjemite into the contaminant mix reproduces the higher Zr/Sm ratio of the Opatica rocks. Lower amounts (2–8%) of assimilation produce *primi-*

Table 3 Parameters used in trace element modelling

	Nb	La	Ce	Nd	Zr	Sm	Eu	Ti	Gd	Dy	Er	Yb
Partition coefficients												
Olivine	0	0.000007	0.00001	0.00007	0.004	0.001	0.001	0.015		0.004	0.009	0.014
Orthopyroxene	0.0013	0.0025	0.005	0.01	0.024	0.02	0.03	0.1		0.05	0.07	0.09
Clinopyroxene	0.0067	0.06	0.1	0.2	0.12	0.3	0.37	0.35		0.44	0.43	0.41
Garnet	0.03	0.0035	0.008	0.05	0.4	0.22	0.45	0.16		2	3.5	5
Values normalised against primitive mantle												
Crustal components												
Average Archaean crust		21.83	17.46	11.83	8.93	7.66	6.55	4.72	5.37	4.88	4.58	4.46
Average Pilbara	11.36	57.87	36.57	21.44	16.52	10.43	5.65	1.56	6.16	3.53	2.96	2.68
Craton granite												
Average Arcahaen trondhjemite	2.53	7.05	5.24	3.17	7.32	1.76	1.77	0.66	1.09	0.59	0.45	0.42
Average adakite	11.64	25.47	19.44	14.84	10.45	6.98	5.77	2.88	3.78	1.94	2.40	1.84
Primitive magmas												
Abitibi	0.59	0.72	0.75	0.82	1.07	0.88	0.86	0.83	1.31	1.80	2.75	3.02
Isua	0.21	0.55	0.57	0.63	1.16	0.83	0.83	0.99	1.29	1.59	2.50	2.41
Whundo	1.12	3.17	2.47	1.93	1.43	1.31	1.43	1.37	1.22	1.07	1.27	1.58
Opatica	0.42	3.20	2.54	1.92	2.32	1.82	1.96	1.75	2.09	2.43	2.56	2.82
Barberton	2.06	5.52	4.39	2.83	3.06	2.18	1.90	1.46	2.15	2.83	3.40	3.71
Mallina Basin	2.13	8.95	7.08	4.20	3.66	2.57	2.02	1.32	1.74	2.16	2.75	3.37
Whundo-type												
Refractory-mantle melt	0.14	0.16	0.20	0.23	0.28	0.36	0.45	0.54	0.70	0.95	1.50	2.03
Whitney-type												
Refractory-mantle melt	0.28	0.32	0.36	0.41	0.46	0.52	0.59	0.68	0.79	0.94	1.12	1.42

Partition coefficients, other than Nb, from Suhr et al. (1998). Partition coefficient for Nb from run 1,802 of Green et al. (2000). Average Archaean crust is from Taylor and McLennan (1985). Average Pilbara Craton granite is from > 1,000 analyses Geoscience Australia and Geological Survey of Western Australia, unpublished data. Average trondhjenmite was determined using analyses from Barker et al. (1979), Davis et al. (1994) and Li and Li (2003). Average adakite is taken from Drummond et al. 1996). Derivation of refractory-mantle melts is outlined in the text

Table 4 Details of trace element modelling

Assimilation/mixing models						
Model (Fig. 10)	Modelled type	Parent magma	Contaminant	Percentage assimilated	F (proportion of melt remaining)	Fractionating assemblage
1	Whitney	Whitney		0	0.3	Cpx
2	Whundo	Whundo	Average Archaean crust	15	1.0	
3	Whundo	Whundo	50% adakite; 50% trondhjemite	8	0.5	ol (60%); opx (40%)
4	Whundo	Whundo	Average Pilbara granite	2	0.5	ol (50%); opx (50%)
5	Whundo	Whundo	Adakite	5	0.5	ol (60%); opx (40%)
6	Mallina, Barberton	Whitney	Average Pilbara granite	5	0.5	ol (50%); opx (50%)
7	Mallina, Barberton	Whundo	Average Pilbara granite	5	0.5	ol (50%); opx (50%)

ol olivine, *opx* orthopyroxene, *cpx* clinopyroxene

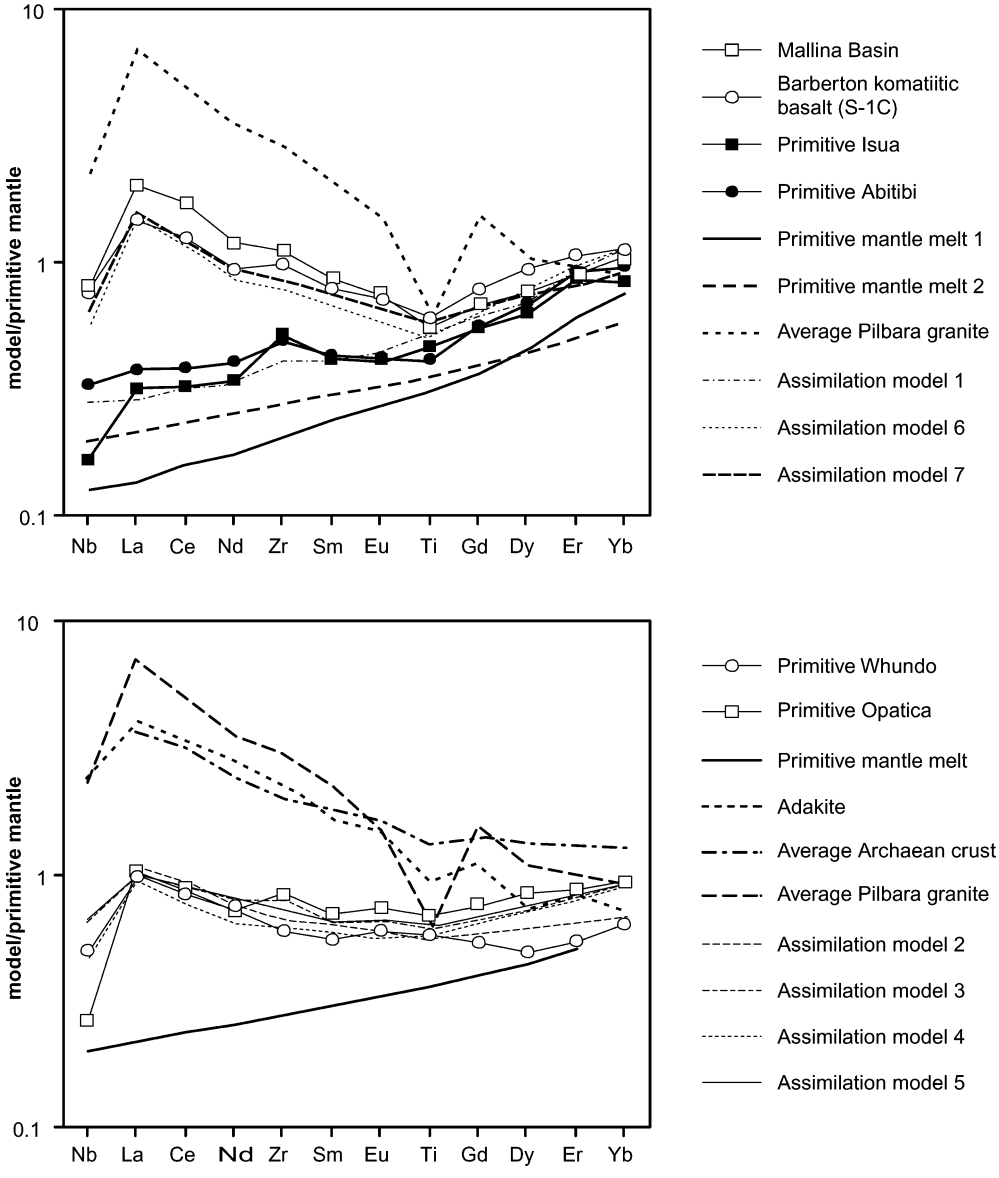

Fig. 10 Primitive mantle normalized trace element diagram showing results of assimilation (and AFC) models. Table 3 presents modeling parameters while individual models are described in Table 4 (primitive mantle normalizing factors of Sun and McDonough 1989)

tive Whundo-type trace element patterns, but only when followed by extensive (~50%) fractional crystallisation of olivine and orthopyroxene (models 3–5, Fig. 10), and this is not consistent with $Mg^{\#}$ as high as 70 for these rocks. Importantly, extensive SHRIMP dating of zircons from comagmatic felsic volcanic units within the

Whundo Group (Nelson 1996, 1997, 1998) found very little evidence (1 "old" zircon out of 145 analyses) for the existence of earlier felsic crust, at least at and above the crustal level at which the felsic magmas evolved. Also, radiogenic Nd-isotopic compositions for the Whundo Group ($\epsilon_{Nd} \sim +2.0$, R.H. Smithies and D.C. Champion, unpublished data) cannot accommodate the assimilation of REE-rich felsic material required by the models. An exception here would be assimilation of more or less contemporaneous felsic material, although Whundo Group felsic volcanics have high concentrations of HREE (Yb >7 ppm) and are compositionally unsuitable contaminants.

Normalised trace element patterns for the Mallina and Barberton second-stage melts can be very closely modelled by contaminating a hypothetical refractory-mantle melt with ~5–10% of either adakitic material or average Pilbara granite (models 6–7, Fig. 10). However, up to ~50% fractional crystallisation of olivine and orthopyroxene is required to achieve the high trace element concentrations of these second-stage melts, depending upon the assumed concentrations in the hypothetical refractory-mantle melt. Recent studies show that the Mallina second-stage melts form a component of the "Mallina mafic suite" (Smithies et al., in press). This suite of compositionally diverse mafic rocks, unified by constant trace element ratios (La/Sm, La/Zr), is interpreted to reflect derivation from a mantle source previously enriched via a subducted sediment component. A similar model might be applicable to the Barberton rocks.

A general conclusion is that the LREE and Th enrichments observed in Archaean second-stage melts is in most cases unlikely to have resulted through assimilation of felsic crust. The alternative hypothesis, an enriched mantle source, draws strong support in some cases (e.g., Abitibi, Opatica, Whundo) from independent geological and geochemical evidence for either an oceanic or subduction setting.

Petrogenesis

Whundo-type rocks

From the previous discussions, several constraints can be placed on the petrogenesis of these rocks. High Al_2O_3/TiO_2, low Gd/Yb, and very low MREE, Ti and HREE concentrations reflect a mantle source considerably more depleted than NMORB source (Fig. 4). Low Gd/Yb, high Al_2O_3 and high-Sc concentrations suggest this refractory source re-melted at pressures low enough that garnet was not stable. Enrichments in Th, U, and LREE, which cannot be accounted for via assimilation of crust, point to mantle-source enrichment. An arc-like magmatic association (tholeiite, calc-alkaline andesite, non-continental sediments) is consistent with the suggestion that mantle enrichment occurred in a subduction-related setting. These rocks also share particularly close compositional similarities with modern boninites in terms of critical features such as Yb/Sc, Gd/Yb, La/Gd ratios.

We propose that the most primitive of the Whundo-type Archaean second-stage melts resulted from melting of a refractory source contaminated by addition of a minor subduction-derived component, leaving a garnet-free residue. The highly variable Zr/Sm ratio of the resulting magma was dependent upon the amount of hornblende and, to a lesser extent, clinopyroxene that was residual in the oceanic slab from which the enriched component was derived. In view of the significant enrichments in Th and Zr, this slab component was likely a melt. Large variations in ratios such as La/Yb, with comparatively little change in $Mg^{\#}$, suggest that much of the compositional variation between the Whundo-type rocks is a result of varying degree of source (re)melting. Compositional variation in source components and fractional crystallisation dominated primarily by olivine and orthopyroxene may have had secondary affects.

Whitney-type rocks

For the Whitney-type second-stage melts, the very low Gd/Yb at unusually high Yb indicates a distinct source component, or mineralogy, unlike that related to the Whundo-types.

We suggest that the petrogenesis of the Whitney-type rocks differs from that of the Whundo-type in two essential ways. First, typically higher Yb, Sc and Al_2O_3 concentrations, higher Yb/Sc and lower Gd/Yb ratios of the Whitney-type rocks are consistent with melting of a refractory source that, at some stage prior to second melting, was very garnet-rich—more so than the source for the Whundo-type rocks. Second, the relatively low La/Yb, La/Nd and La/Sm ratios of the Whitney-type limit the amount of possible enrichment (either of the source or through assimilation), although normalised trace element patterns show that some has clearly occurred.

There is a very close association between the Whitney-type rocks and ultramafic magmas, including komatiites, which suggests a strong and possibly genetic link with a mantle plume (e.g., Kerrich et al. 1998). What is unclear is whether a plume simply added the heat required to melt a refractory mantle source near the base of the lithosphere, or represented an actual source component of the Whitney-type rocks. Either way, there is no obvious requirement that the refractory source had also been subduction modified, or fluxed.

Independent evidence for a subduction setting for the Whitney-type rocks from Isua is difficult to evaluate due to extreme deformation, although it has been suggested (Polat et al. 2002). The Abitibi second-stage melts, however, do appear to be associated with magmatic successions that are consistent with an oceanic subduction-related setting (e.g., Kerrich et al. 1998; Polat and

Kerrich 2001; Wyman et al. 2002) and our trace element modelling supports the suggestion that the Abitibi rocks have not directly assimilated felsic crust. While these second-stage melts have unusually low La/Nb and Th/Nb ratios, some modern arc volcanics derived from mantle sources thought to have been metasomatised solely through interaction with slab-derived fluids can have highly incompatible trace element patterns generally similar to those of the Abitibi second-stage melts (e.g., Woodhead et al. 1998). Plume induced melting of a previously garnet-rich, refractory mantle that was more (Isua) or less (Abitibi) modified by subduction-related fluids remains a possible petrogenetic model for Whitney-type magmas.

The Barberton and Mallina second-stage melts

The Barberton komatiitic basalts and the Mallina second-stage melts have very similar trace element patterns with Gd/Yb ratios transitional between the Whundo- and Whitney-type rocks. Unlike the Whundo-type rocks, the Barberton rocks are associated with a volcanic sequence containing abundant komatiite, komatiitic basalt and tholeiitic basalt. In terms of this association, they are more like the Whitney-type. They are very rare compared to the associated komatiites and other komatiitic basalts in the succession (Jahn et al. 1982; Parman et al. 2001). These more abundant rocks typically have $[Gd/Yb]_{PM} > 1.0$ (Sun and Nesbitt 1978; Jahn et al. 1982; Parman et al. 2001; Arndt 2003a) and cannot be related to the LREE-rich second-stage melts through any simple liquid line of descent. Our trace element modelling also suggests that the differences between the Barberton second-stage melts and the other Barberton komatiitic basalts is unlikely to relate alone to mantle source contamination or assimilation of felsic crust—although either or both of these magmas may form in this way from unrelated parental magmas. The petrogenesis of the Barberton second-stage melts is particularly difficult to determine and a subduction-enriched source can be neither supported nor ruled out on present evidence.

The Mallina second-stage melts form a component of the "Mallina mafic suite" a compositionally diverse and geographically extensive suite unified by consistent La/Sm, La/Nb, and La/Zr ratios that cannot be explained via assimilation of the highly heterogeneous Pilbara crust (Smithies et al. in press). They most likely reflect derivation from a mantle source previously enriched via a subduction component dominated by melts derived from a felsic sedimentary source. Smithies (2002) and Smithies et al. (in press) speculate that this subduction-modified source lay inert for between 50 and 160 m.y. before being re-melted. A similar petrogenetic model may also apply to the compositionally similar Barberton komatiitic basalts. Although numerous independent lines of evidence suggest a regional thermal anomaly centred on the Pilbara Craton more or less contemporaneous with formation of the Mallina second-stage melts (Smithies and Champion 2000), it is unclear whether this was a result of a plume, delamination, or rapid crustal extension. In the case of the Barberton komatiitic basalts, a plume-related heat source certainly seems highly likely.

Discussion: boninitic or not?

Archaean LREE-enriched second-stage melts show several subtle to more obvious compositional differences with modern boninites, in particular in having lower SiO_2 and higher Al_2O_3 and HREE; and so none may adhere to a *strict* definition of boninite (e.g., Crawford et al. 1989). Nevertheless, despite these compositional differences, it is clear that Archaean second-stage melts, and particularly the Whundo-type, also broadly comply with a boninitic paragenesis in that they formed through relatively low-pressure melting of a strongly refractory source that was re-enriched prior to melting, in what (in many cases) seems likely to have been a subduction-environment.

Many of these Archaean second-stage melts can be accommodated within a broader definition of a boninitic petrogenesis that takes into consideration the likely secular changes in mantle and crustal composition and pressure and temperature regime from Archaean to present.

An implication from the relative concentrations of Sc, V, HREE and Al_2O_3, and from Gd/Yb ratios is that the petrogenesis of all Archaean second-stage melts involved more garnet than has been the case for modern boninites. This is particularly so for the Whitney-type rocks; the Whundo-type have Gd/Yb, Yb and Al_2O_3 values between those of the Whitney-type and modern boninites (Figs. 3 and 5). A garnet-rich petrogenesis might have resulted from higher mantle potential temperatures, which are widely thought to have exceeded present temperatures by up to 150°C (e.g., Davies 1995; Ohta et al. 1996). In a hotter Archaean asthenosphere, decompression melting would have typically begun at a greater pressure than it does today, with the increased likelihood of a garnet-bearing residue. For Archaean second-stage melts, it is most likely that this garnet was residual from an early melt-depletion event, but was subsequently eliminated during, or before, second melting.

Consequently, we propose that the Whundo-type second-stage melts are very close Archaean analogues of modern boninites, essentially differing only in that the Archaean source contained slightly more garnet prior to remelting.

The close association between calc-alkaline volcanic rocks and plume-related komatiitic magmatism has been used to develop a model of subduction zone—plume interaction (Fan and Kerrich 1997; Kerrich et al. 1998; Wyman 1999; Wyman et al. 2002). According to this model, Whitney-type rocks are derived from a subduction-modified refractory mantle wedge, while a plume provides additional heat. Arndt (2003b) questioned the

plausibility of close interaction between a plume and subduction-zone magmatism, suggesting that neither a plume nor related magmas are likely to penetrate an actively subducting slab. Danyushevsky et al. (1995) and Falloon and Danyushevsky (2000), however, provide evidence that such interactions have occurred, and in the case of the Samoan plume and the Lau Basin at the northern end of the Tongan subduction zone, have produced a range of magmas that include high-Ca boninites and ocean island basalt. According to these authors, the Samoan plume has penetrated the mantle wedge above the subducting Pacific plate along a strike-slip transform plate boundary (Danyushevsky et al. 1995; Falloon and Danyushevsky 2000). The plume has melted to form ocean island basalt and the residue from this melting has been subsequently metasomatised by slab fluids and remelted to produce the Tongan high-Ca boninites. It is also proposed that the extension caused by slab rollback may draw a plume (or part of it) into a mantle wedge (Danyushevsky et al. 1995). Interestingly, Danyushevsky et al. (1995) also argued that the Tongan boninitic magmas have variably mixed with ocean island basalt magmas that resulted from earlier melting within the plume, producing additional enrichments in LREE and Nb concentrations within the boninites. A similar process would certainly explain the low La/Nb and Th/Nb ratios of the Abitibi second-stage melts, and because such magma mixing is not a *necessary* feature, the plume-subduction zone interaction model, as applied by Danyushevsky et al. (1995), can also accommodate the significantly higher La/Nb ratios of the Archaean Isua rocks. According to Falloon and Danyushevsky (2000), high-Ca boninites require melting temperatures around 1,480°C and hence upwelling of a deep mantle source component. If this is the case, a plume source, and hence plume-subduction zone interaction, is a general requisite for high-Ca boninite magmatism.

If the Whitney-type rocks are indeed subduction related (Kerrich et al. 1998; Wyman et al. 2002; Polat et al. 2002), then their petrogenesis might resemble that of modern high-Ca boninites despite the obvious compositional differences between the two types of rocks—which we suggest primarily relates to a more garnet-rich source at some stage in the petrogenesis of the Whitney-type rocks. Whitney-type rocks also have significantly lower La/Yb ratios than modern high-Ca boninites. This might reflect very inefficient subduction enrichment processes (Kerrich et al. 1998), at least during some (earlier?) styles of Archaean subduction, perhaps linked in some way to the more buoyant nature of Archaean oceanic crust that was likely to be *at least* twice as thick as modern oceanic crust (15–20 km, e.g., Ohta et al. 1996).

Conclusions

Rare Archaean second-stage melts that show a range of compositional features in common with modern boninite can be divided into at least two distinct groups, termed here the Whundo-type and the Whitney-type. The Whundo-type second-stage melts are compositionally most like modern boninites and have been found in greenstone successions dated at 3.12 Ga (Whundo, Smithies et al. in preparation) and 2.8 Ga (Opatica, Boily and Dion 2002). These successions are dominated by tholeiitic to calc-alkaline mafic to intermediate volcanic rocks that closely resemble successions found at modern arcs (Boily and Dion 2002; Smithies et al., in preparation). The Whundo-type rocks differ compositionally from modern boninites in ways that can be adequately accounted for through secular changes in the thermal regime in the mantle, which predict more common garnet-rich residual sources in the Archaean. We propose that the Whundo-type rocks are true Archaean analogues of modern boninites.

The Whitney-type rocks occur throughout the Archaean and are closely associated with ultramafic magmatism including komatiites in an affiliation unlike that of modern subduction zones. They are characterised by extremely depleted compositions that require a source more garnet-rich than the source for either modern boninites or Whundo-type second-stage melts. Trace element modelling provides few practical constraints on the origins of these rocks, which may be a result of a range of different processes and/or source components. Nevertheless, their petrogenesis appears either directly or indirectly related to plume magmatism. Plausible petrogenetic models include: (1) crustal (though not felsic) contamination of a strongly depleted magma derived from a plume source, (2) plume-induced melting of subduction modified refractory mantle, (3) local fluxing of refractory plume source by subduction-derived fluids. A plume component, like that proposed for the Tongan high-Ca boninites, provides an explanation for the low La/Nb and Th/Nb ratios in the Abitibi rocks, the apparent oceanic setting of which precludes the possibility that trace-element enrichment relates to assimilation of felsic crust (e.g., Kerrich et al. 1998).

The Mallina and Barberton second-stage melts cannot be confidently assigned to either the Whundo- or Whitney-type. The Barberton rocks, like the Whitney-type, are closely associated with komatiites and may relate in some way to mantle plume magmatism. If they are subduction related, then their high-La/Yb ratios may indicate mantle-source metasomatism involving an adakitic slab-melt, rather than a fluid. However, crustal assimilation of a refractory-mantle melt remains a plausible explanation. A petrogenesis like that proposed for the geochemically similar Mallina second-stage melts also cannot be ruled out.

If the Whundo-type rocks are true Archaean analogues of modern boninites, then the suggestion that the Whitney-type rocks may also have had a boninitic petrogenesis implies a wide range of conditions and of compositional components forming boninites, albeit apparently very rarely, in the Archaean. A plume-related (or at least influenced) model, similar in some regards to

that suggested for the modern Tongan high-Ca boninites (Danyushevsky et al. 1995), might apply to the Whitney-type rocks, although the source compositions and source enrichment processes appear more uniquely Archaean. The Whundo-type rocks show that plate tectonic processes essentially the same as those that produce modern boninites have operated since ~3.12 Ga.

Acknowledgements We thank Paul Morris, Steve Parman, Steve Sheppard and an anonymous reviewer for many constructive suggestions. Steve Parman kindly provided us with an unpublished analysis of a komatiitic basalt from Barberton. Louise Fogarty is thanked for drafting the figures. Published with the permission of the Director, Geological Survey of Western Australia and the Chief Executive Officer, Geoscience Australia.

References

Abbott DH, Hoffmann SE (1984) Archean plate tectonics revisited: 1. Heat flow, spreading rate, and the age of subducting oceanic lithosphere and their effects on the origin and evolution of continents. Tectonics 3:429–448

Arndt N (2003a) Komatiites, kimberlites, and boninites. J Geophy Res 108. DOI:10.1029/2002JB002157

Arndt N (2003b) Komatiites and island arc volcanics in Archean greenstone belts: biased preservation of a rare magmatic association. Eur Geophy Soc Geophy Res Abs 5, 06684

Arndt NT, Jenner GA (1986) Crustally contaminated komatiites and basalts from Kambalda, Western Australia. Chem Geol 56:229–255

Arndt NT, Albarede F, Cheadle MM, Ginibre C, Herzberg C, Jenner G, Chauvel C, Lahaye Y (1998) Were komatiites wet? Geology 26:739–742

Barker F, Millard HT Jr, Lipman PW (1979) Four low-K siliceous rocks of the western USA. In: Barker F (ed) Trondhjemites, dacites, and related rocks (Developments in Petrology 6), Elsevier, Amsterdam

Barley ME (1986) Incompatible-element enrichment in Archaean basalts: a consequence of contamination by older sialic crust rather than mantle heterogeneity. Geology 14:947–950

Bickle MJ (1986) Implications of melting for stabilisation of the lithosphere and heat loss in the Archaean. Earth Planet Sci Lett 80:314–324

Boily M, Dion C (2002) Geochemistry of boninite-type volcanic rocks in the Frotet-Evans greenstone belt, Opatica subprovince, Quebec: implications for the evolution of Archaean greenstone belts. Precambrian Res 115:349–371

Cadman AC, Tarney J, Hamilton MA (1997) Petrogenetic relationships between Palaeoproterozoic tholeiitic dykes and associated high-Mg noritic dykes, Labrador, Canada. Precambrian Res 82:63–84

Cameron WE, McCulloch MT, Walker DA (1983) Boninite petrogenesis: chemical and Nd-Sr isotopic constraints. Earth Planet Sci Lett 65:75–89

Crawford AJ, Falloon TJ, Green DH (1989) Classification, petrogenesis and tectonic setting of boninites. In: Crawford AJ (ed) Boninites. Unwin-Hyman, London, pp 1–49

Danyushevsky LV, Sobolev AV, Falloon TJ (1995) North Tongan high-Ca boninite petrogenesis: the role of Samoan plume and subduction zone-transform fault transition. J Geodyn 20:219–241

Davies GF (1995) Punctuated tectonic evolution of the earth. Earth Planet Sci Lett 36:363–380

Davis WJ, Fryer BJ, King JE (1994) Geochemistry and evolution of Late Archean plutonism and its significance to the tectonic development of the Slave craton. Precambrian Res 67:207–241

DePaolo DJ (1981) Trace element and isotopic effects of combined wallrock assimilation and fractional crystallisation. Earth Planet Sci Lett 53:189–202

Drummond MS, Defant MJ, Kepezhinskas PK (1996) Petrogenesis of slab-derived trondhjemite-tonalite-dacite/adakite magmas. Trans R Soc Edinb Earth Sci 87:205–215

Falloon TJ, Crawford AJ (1991) The petrogenesis of high-calcium boninite lavas dredged from the northern Tonga ridge. Earth Planet Sci Lett 102:375–394

Falloon TJ, Danyushevsky LV (2000) Melting of refractory mantle at 1.5, 2 and 2.5 GPa under anhydrous and H_2O-undersaturated conditions: implications for the petrogenesis of high-ca boninites and the influence of subduction components on mantle melting. J Petrol 41:257–283

Fan J, Kerrich R (1997) Geochemical characteristics of aluminium depleted and undepleted komatiites and HREE-enriched low-Ti tholeiites, western Abitibi greenstone belt: a heterogeneous mantle plume-convergent margin environment. Geochim Cosmochim Acta 61:4723–4744

Gaetani Ga, Kent AJR, Grove TL, Hutcheon ID, Stolper EM (2003) Mineral/melt partitioning of trace elements during hydrous peridotite partial melting. Contrib Mineral Petrol 145:391–405

Gamble JA, Wright IC, Woodhead JD, McCulloch MT (1995) Arc and back-arc geochemistry in the southern Kermadec arc-Ngatoro Basin and offshore taupo Volcanic Zone, SW Pacific. In: Smellie JL (ed) Volcanism associated with extension at consuming plate margins. Geol Soc Lond Spec Pub 81:193–212

Green TH, Blundy JD, Adam J, Yaxley GM (2000) SIMS determination of trace element partition coefficients between garnet, clinopyroxene and hydrous basaltic liquids at 2–7.5 Gpa and 1,080–1,200°C. Lithos 53:165–187

Hall RP, Hughes DJ (1993) Early Precambrian crustal development: changing styles of mafic magmatism. J Geol Soc Lond 150:625–635

Hawkesworth CJ, Gallagher K, Hergt JM, McDermott F (1993a) Trace element fractionation processes in the generation of island arc basalts. Phil Trans R Soc Lond Series A 342:179–191

Hawkesworth CJ, Gallagher K, Hergt JM, McDermott F (1993b) Mantle and slab contributions in arc magmas. Ann Rev Earth Planet Sci 21:175–204

Hickey RL, Frey RA (1982) Geochemical characteristics of boninite series volcanics: implications for their source. Geochim Cosmochim Acta 46:2099–2115

Hickman AH (1997) A revision of the stratigraphy of Archaean greenstone successions in the Roebourne-Whundo area, west Pilbara: Geol Surv West Aust Ann Rev 1996–1997:76–82

Hollings P, Kerrich R (1999) Trace element systematics of ultramafic and mafic volcanic rocks from the 3 Ga North Caribou greenstone belt, northwestern Superior Province. Precambrian Res 93:257–279

Hollings P, Wyman D, Kerrich R (1999) Komatiite-basalt-rhyolite volcanic associations in Northern Superior Province greenstone belts: significance of plume-arc interaction in the generation of the proto continental Superior Province. Lithos 46:137–161

Jahn BM, Gruau G, Glikson AY (1982) Komatiites of the onverwacht group, S. Africa: REE geochemistry, sm/nd age and mantle evolution. Contrib Mineral Petrol 80:25–40

Kerrich R, Wyman D, Fan J, Bleeker W (1998) Bonninite series: low-Ti tholeiite associations from the 2.7 Ga Abitibi greenstone belt. Earth Planet Sci Lett 164:303–316.

Li W-X, Li X-H (2003) Adakitic granites within the NE Jiangxi ophiolites, South China: geochemical and Nd isotopic evidence. Precambrian Res 122:29–44

Martin H (1999) Adakitic magmas: modern analogues of Archaean granitoids. Lithos 46:411–429

Nelson DR (1996) Compilation of SHRIMP U-Pb zircon geochronology data, 1995. W Aust Geol Surv Record 1996/2

Nelson DR (1997) Compilation of SHRIMP U-Pb zircon geochronology data, 1996. W Aust Geol Surv Record 1997/2

Nelson DR (1998) Compilation of SHRIMP U-Pb zircon geochronology data, 1997. W Aust Geol Surv Record 1998/2

Ohta H, Maruyama S, Takahashi E, Watanabe Y, Kato Y (1996) Field occurrence, geochemistry and petrogenesis of the Archean mid-oceanic ridge basalts (AMORBs) of the Cleaverville area, Pilbara Craton, Western Australia. Lithos 37:199–221

Parman SW, Grove TL, Dann JC (2001) The production of Barberton komatiites in an Archean subduction zone. Geophy Res Lett 28:2513–2516

Parman SW, Shimizu N, Grove TL, Dann JC (2003) Constraints on the pre-metamorphic trace element composition of Barberton komatiites from ion probe analyses of preserved clinopyroxene. Contrib Mineral Petrol 144:383–396

Piercey SJ, Murphy DC, Mortensen JK, Paradis S (2001) Boninitic magmatism in a continental margin setting, Yukon-Tanana terrane, southeastern Yukon, Canada. Geology 29:731–734

Polat A, Kerrich R (2001) Magnesian andesites, Nb-enriched basalt-andesites, and adakites from late-Archean 2.7 Ga Wawa greenstone belts, Superior Province, Canada: implication for late Archean subduction zone petrogenetic processes. Contrib Mineral Petrol 141:36–52

Polat A, Hofmann AW, Rosing MT (2002) Boninite-like volcanic rocks in the 3.7–3.8 Ga Isua greenstone belt, West Greenland: geochemical evidence for intra-oceanic subduction zone processes in the early earth. Chem Geol 184:231–254

Riganti A (1996) The northern segment of the early Archaean Nondweni greenstone belt, South Africa—field relations and petrogenetic constraints. PhD Thesis (unpublished), University of Natal

Riganti A, Wilson AH (1995) Geochemistry of the mafic/ultramafic volcanic associations of the Nondweni greenstone belt, South Africa, and constraints on their petrogenesis. Lithos 34:235–252

Smith JB (2003) The episodic development of intermediate to silicic volcano-plutonic suites in the Archaean West Pilbara, Australia. Chem Geol 194:275–295

Smithies RH (2002) Archaean boninite-like rocks in an intracratonic setting. Earth Planet Sci Lett 197:19–34

Smithies RH, Champion DC (2000) The Archaean high-Mg diorite suite: links to tonalite-trondhjemite-granodiorite magmatism and implications for early Archaean crustal growth. J Petrol 41:1653–1671

Smithies RH, Champion DC, Sun S-S Evidence for early LREE-enriched mantle source regions: diverse magmas from the ca. 3.0 Ga Mallina Basin, Pilbara Craton, NW Australia. J Petrol (in press)

Suhr G, Seck HA, Shimizu N, Gunther D, Jenner G (1998) Infiltration of refractory melts into the lowermost oceanic crust: evidence from dunite- and gabbro-hosted clinopyroxenes in the Bay of Island Ophiolites. Contrib Mineral Petrol 131:136–154

Sun S-S, Nesbitt RW (1978) Geochemical regularities and genetic significance of ophiolitic basalts. Geology 6:689–693

Sun S-S, McDonough WF (1989) Chemical and isotopic systematics of oceanic basalts: implications for mantle compositions and processes. In: Saunders AD, Norry, MJ (eds) Magmatism in ocean basins. Geol Soc Lond Spec Pub 42:313–345

Sun S-S, Nesbitt RW, McCulloch MT (1989) Geochemistry and petrogenesis of Archaean and early Proterozoic siliceous high-magnesian basalts. In: Crawford AJ (ed) Boninites. Unwin-Hyman, London, pp 149–173

Tarney J (1992) Geochemistry and significance of mafic dyke swarms in the Proterozoic, In: Kondie KC (ed) Proterozoic crustal evolution, Elsevier, Amsterdam, pp 151–179

Taylor SR, McLennan SM (1985) The continental crust: its composition and evolution. Blackwell, Oxford

Wilson AH (2003) A new class of silica-enriched, highly depleted komatiites in the southern Kaapvaal Craton, South Africa. Precambrian Res 127:125–141

Wilson AH, Shirey SB, Carlson RW (2003) Archaean ultra-depleted komatiites formed by hydrous melting of cratonic mantle. Nature 423:858–861

Woodhead JD, Eggins S, Gamble JA (1993) High field strength and transition element systematics in island arc and back-arc basin basalts: evidence for multi-stage melt extraction and an ultra-depleted mantle wedge. Earth Planet Sci Lett 114:491–504

Woodhead JD, Eggins SM, Johnson RW (1998) Magma genesis in the New Britain Island arc: further insights into melting and mass transfer processes. J Petrol 39:1641–1668

Wyman DA (1999) A 2.7 Ga depleted tholeiite suite: evidence of plume-arc interaction in the Abitibi greenstone belt, Canada. Precambrian Res 97:27–42

Wyman DA, Kerrich R, Polat A (2002) Assembly of Archean cratonic mantle lithosphere and crust: plume-arc interaction in the Abitibi-Wawa subduction-accretion complex. Precambrian Res 115:37–62